Available online at www.sciencedirect.com

SciVerse ScienceDirect

Ceramics International 39 (2013) 5295–5302

CERAMICS INTERNATIONAL

www.elsevier.com/locate/ceramint

Fabrication and characterization of reaction-bonded silicon carbide with poly(methyl methacrylate) as pore-forming agent

Qide Wu[a], Chaochen Yang[a], Hongquan Zhang[a,b,*], Changxia Yin[a], B.W. Darvell[c], Xia Fan[a]

[a]*Silicate Materials Engineering Research Center, Wuhan University of Technology, Wuhan, China*
[b]*School of Materials Science and Engineering, Wuhan University of Technology, Wuhan, China*
[c]*Dental Materials Science, Faculty of Dentistry, Kuwait University, Kuwait*

Received 29 August 2012; received in revised form 10 December 2012; accepted 10 December 2012
Available online 20 December 2012

Abstract

Reaction-bonded silicon carbide (RBSC) ceramics were prepared by liquid silicon infiltration at 1600 °C using a carbon biscuit. The green body was made by slip casting a stabilized carbon powder slurry, followed by pyrolysis in a vacuum furnace at 1000 °C for 2 h; the density of the biscuit (ρ_b) was controlled using poly(methyl methacrylate) (PMMA) powder as pore former in mass proportion from 30% to 50% in 5 percentage point intervals. The particle size of the PMMA had significant effects on the microstructure, distribution of residual silicon, and the mechanical properties of the ceramic. For 40 mass% PMMA with $d_{50}=1.17$ μm and $d_{50}=0.51$ μm, ρ_b was 0.81 and 0.82 g/mL, with corresponding biscuit porosities of 51% and 50%, which gave peak values of both RBSC ceramic density of 3.07 and 3.10 g/mL, and flexural strength of 741 and 794 MPa, respectively. XRD analysis showed that the main phase was β-SiC, with a small quantity of α-SiC. Using PMMA with $d_{50}=0.51$ μm, a small quantity of residual Si was well dispersed with grain size <1 μm. "Black core" residual carbon in the RBSC was successfully avoided when $\rho_b \leq 0.82$ g/mL (mass proportion PMMA $\geq 35\%$). PMMA as pore former favored the elimination of the detrimental black core and the preparation of dense RBSC with good mechanical properties.

Keywords: A. Reactive sintering; C. Mechanical properties; D. Silicon carbide; PMMA

1. Introduction

The best way to fabricate silicon carbide (SiC) ceramics is considered to be direct reaction *in situ* by infiltration of pure carbon biscuits with molten silicon at low temperature (1450–1600 °C) to produce so-called reaction-bonded silicon carbide (RBSC) [1–5]. Compared with other sintering techniques, such as hot-pressing, liquid-phase, pressless and air-press sintering, such a technique is favorable for near-net shape fabrication of large and complex parts, without the use of additives, obtaining an almost fully-dense product. Moreover, such ceramics have excellent flexural strength at temperatures lower than 1380 °C [2].

High strength RBSC ceramics have been sought for some years. Suyama et al. [2] found that flexural strength was improved by decreasing the particle size of the raw powders, attaining 1070 MPa when the particle size of residual silicon was under 100 nm, but the shaping process was complicated. While fine acicular β-SiC has been used to reinforce RBSC ceramics [6,7], the density and microstructure of carbon biscuits have been found to be the main influencing factors for infiltrated materials [8–10]. Chiang et al. [8] obtained a porous pure carbon biscuit by means of polymer pyrolysis and carbonization according to the Hucke method [9], giving a flexural strength over 1 GPa after liquid silicon infiltration. Wood blocks can also be converted to porous, pure carbon biscuits by carbonization, giving a flexural strength after liquid silicon infiltration of some 200–700 MPa [10–14]. However, uniform porosity has not been possible using wood [7,8,11,12,14], with the carbon density, $\rho_b > 0.96$ g/mL (*cf.* the ideal figure, Section 3.6, below) in some parts of

*Corresponding author at: School of Materials Science and Engineering, Wuhan University of Technology, No. 122 Luoshi Road, Wuhan 430070, Hubei China. Tel.: +86 87651779; fax: +86 87213139.
E-mail addresses: zhhquan@hotmail.com, zhq-wh@126.com (H. Zhang).

0272-8842/$ - see front matter © 2012 Elsevier Ltd and Techna Group S.r.l. All rights reserved.
http://dx.doi.org/10.1016/j.ceramint.2012.12.032

the biscuit, preventing full infiltration [15]. This residual carbon "black core" in the RBSC was found to be one of the main reasons for the poor strength, but no means of eliminating this has been reported. In unpublished preliminary work, we found that residual carbon in the resulting RBSC ceramic could be reduced to 0.08 mass% by using carbon biscuits prepared with PMMA microbeads as pore former, essentially solving the problem.

In this paper, we formalize that result, assessing the effects of particle size and proportion of PMMA, focusing on the occurrence of residual carbon and the relationship of the density of the carbon biscuit to the resulting RBSC properties.

2. Experimental procedure

2.1. Synthesis of PMMA and its size distribution

PMMA powders were prepared according to the methods of Chen et al. [16] and Gu et al. [17]. Their particle size distributions (Fig. 1) were determined using laser diffraction (Master-sizer 3000, Malvern Instruments, Malvern, Worcestershire, UK). Their median diameters (d_{50}) were 1.17 μm ($P_{1.2}$) and 0.51 μm ($P_{0.5}$), while the proportions of particles with a size ≥ 2 μm were about 11.3% and 4.6%, respectively. The size distribution for $P_{0.5}$ was more uniform than that of $P_{1.2}$, which would favor the preparation of RBSC ceramics with more uniform microstructure.

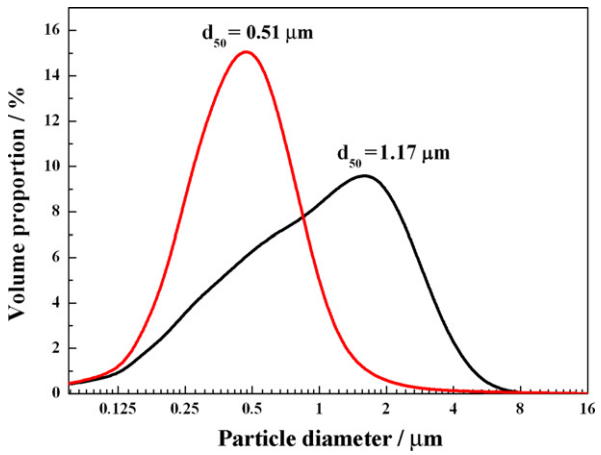

Fig. 1. Particle size distributions of PMMA powders $P_{1.2}$ and $P_{0.5}$.

2.2. Preparation of RBSC

Aqueous suspensions with a total solid proportion of 50–52 vol% were prepared using each of the above PMMAs and a carbon powder (99.99% purity, N774; Carbon JSC, Ivanovo, Ivanovo, Russia) at PMMA: carbon (P: C) mass ratios of 30:70, 35:65, 40:60, 45:55 and 50:50. Poly(vinylpyrrolidone) (K30; ISP, Wayne, NJ, USA) solution (2 mass% in distilled water) was used to disperse the carbon powders before adding the PMMA powder; the pH of the suspension was adjusted to 9.5 using 10% aqueous ammonia (analytical grade, Zhongnan Chemical Reagent, Wuhan, Hubei, China). After adding 0.1–0.5% by mass of defoaming agent (NXZ; San Nopco, Nogaya, Japan), the suspension was stirred with a magnetic bar for 24 h at about 150 r.p.m., then exposed to low pressure (~100 Pa) at ambient temperature (25 ± 3 °C) for 20 min to remove bubbles. The green body, formed by slip casting in a plaster mold of $8 \times 8 \times 60$ mm^3 and drying at 75 °C for 48 h, was heated at ~10 °C/min from ambient to 1000 °C and then held for 2 h in a vacuum furnace at 10–100 Pa. The resulting carbon biscuits were dry ground to $3.5 \times 4.5 \times 46$ mm^3 on 500 grit SiC paper, removing surface dust with an air jet. The silicon powder (purity 99.2 mass%; Zhejiang Kaihua Yuantong Silicon Industry, Kuaihua, Zhejiang, China), with an excess of 5 mass% based on the theoretically calculated value by mass of the biscuit, was then put on the top of the biscuit in a pile (infiltration cannot be complete if there is no excess Si provided with respect to the stoichiometry of SiC since the evaporation rate of molten Si is substantial [18], despite the low vapor pressure [19]). The biscuits were then placed in a graphite resistance-heated furnace (Astro, Thermal Technologies, Santa Barbara, CA, USA) for the silicon to melt, infiltrate by capillarity, and react with the carbon, being heated at ~15 °C/min from ambient to 1600 °C and then held for 2 h under vacuum (~1 Pa). The specimens obtained were finally wet ground on 500 grit SiC paper to remove the excess silicon on the surface, and then dried at 105 °C for 1 h in air before characterization.

2.3. Characterization

The zeta potential of both PMMAs and the carbon powder in distilled water was determined as a function of pH (Zeta PALS, Brookhaven Instruments, Holtsville, NY, USA), using 10% aqueous ammonia or 1 mol/L nitric acid (analytical grade, Sinopharm Chemical Reagent, Shanghai, China) to adjust the pH. The viscosity–shear strain rate behavior of a $P_{1.2}$:C 40:60 suspension at pH 9.5 and a total solid proportion of 52 vol% at 25 °C was determined (4ARES-9a; Rheo-metric Scientific, Piscataway, NJ, USA). The porosity and density of the biscuit and the density of RBSC ceramic, after drying at 105 °C for 1 h, were determined using an Archimedean water-displacement method. The phase description of the products was determined by X-ray diffraction (XRD; PW1710; Philips, Almelo, Holland) using Cu-Kα radiation at 40 kV and 100 mA. To avoid the interference that would occur from carbon- or gold sputter-coating on observation of the microstructure and distribution of residual carbon (C_R) or silicon (Si_R) in the RBSC using scanning electron microscopy (SEM), a metallurgical microscope (BJ-X, Shanghai Batuo Instrument Co, Shanghai, China) was used.

Groups of six rectangular bar specimens of RBSC ceramics ($45 \times 3.5 \times 2.5$ mm^3, ground flat and polished using diamond polishing pastes to 0.5 μm finish on all faces) were tested in three-point bending at a span of

30 mm, with 3 mm diameter supports, and a crosshead speed of 0.5 mm/min on a universal testing machine (AG-2000A, Shimadzu, Kyoto, Japan) at room temperature (25 ± 3 °C). After fracture, the dimensions of the cross-section were measured to ± 0.01 mm using a digital venier caliper (0–150 mm, Shanghai Tool Works, Shanghai, China) to calculate flexural strength (σ_f). The thermal decomposition behavior of the PMMA was determined thermo-gravimetrically in a differential scanning calorimeter (TG–DSC; STA490C, Netzsch-Geratebau, Selb, Germany) up to 800 °C in flowing N_2 at 10 K/min. Adsorbed water was removed by drying at 75 °C for 48 h beforehand.

3. Results and discussion

3.1. Dispersibility of PMMA and carbon powders

Fig. 2(a) shows the zeta potential value of 2 mass% suspensions of $P_{1.2}$ and carbon powders as a function of pH. The isoelectric points were at pH = 4.5 and 5, correspondingly. The maximum absolute values occurred at pH = 9 for PMMA (−27.6 mV) and pH 10 for carbon (−41.3 mV). Given this, dispersions of each PMMA powder with carbon at mass ratios of 30:70, 35:65, 40:60, 45:55 and 50:50 and total solid volume fraction of 52% in distilled water were prepared at pH 9.5. These showed good stability, with no settling being observed over 3 h. The $P_{1.2}$:C 40:60 suspension behaved as a pseudoplastic fluid (Fig. 2(b)), its viscosity decreasing with increasing shear strain rate; at 40 s^{-1} the viscosity was 250 mPa s. Such a suspension was thus well suited to slip casting.

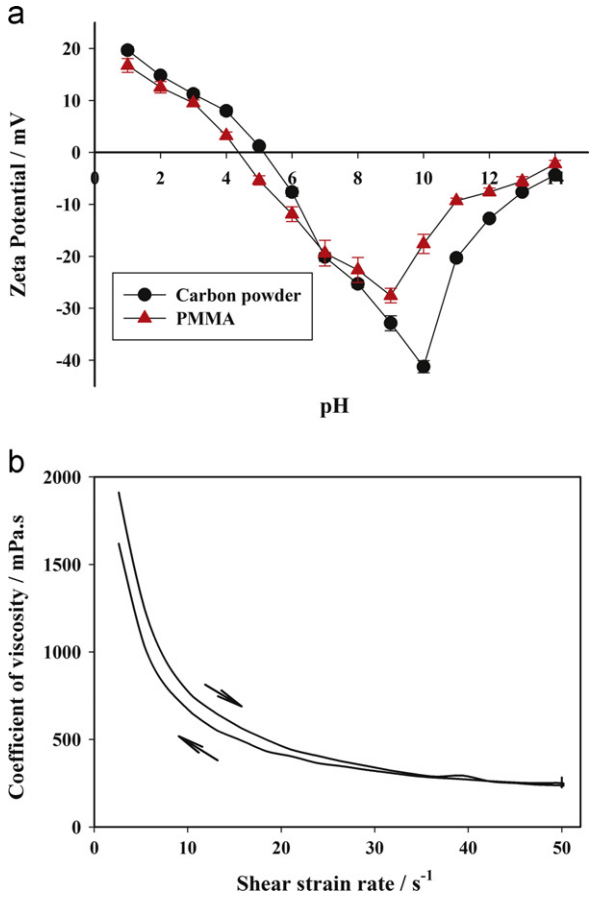

Fig. 2. (a) Zeta potential *vs.* pH for PMMA and carbon powders separately in water and (b) rheological behavior of $P_{1.2}$:C = 40:60 suspension in water.

3.2. Effect of PMMA content on properties of RBSC

Fig. 3 shows a typical XRD pattern for the RBSC product ($P_{1.2}$:C = 40:60) with 3C–SiC (here called β-SiC), and 6H–SiC (α-SiC) and Si identified as the main crystalline phases, calculated from peak intensities to be in the proportions 76:14:10 (mass%) respectively; crystalline carbon was not detectable. Mallick et al. [13] had reported that only β-SiC and Si were present in Si/SiC ceramics, but diffraction peaks for α-SiC were clearly found now. Generally, the reaction Si + C → SiC is exothermic (−360 kJ/mol at > ~1450 °C) [20], and this may have caused local temperatures to exceed 2000 °C, perhaps prompting the phase transformation: β-SiC → α-SiC [21].

The pure carbon biscuits prepared using each PMMA powder suffered a linear shrinkage of ~15% on being pyrolised, although no surface cracks were found. Fig. 4 shows the flexural strength and density of the RBSC ceramics, and the density and porosity of the preceding carbon biscuit. The density of the biscuit ρ_b decreased from ~0.90 to ~0.73 g/mL with the increase of the PMMA content from 30% to 50% in the mixture for both sizes, whereas the porosity of the carbon biscuit (P_C) correspondingly increased nearly linearly from 40% to 61%. The values for ρ_b and P_C were not systematically different by using $P_{1.2}$ and $P_{0.5}$. For the RBSC ceramics, both their density and flexural strength showed a marked maximum value for P:C of 40:60 for both PMMA powders, these values being roughly correlated (Fig. 5). This would be expected since the

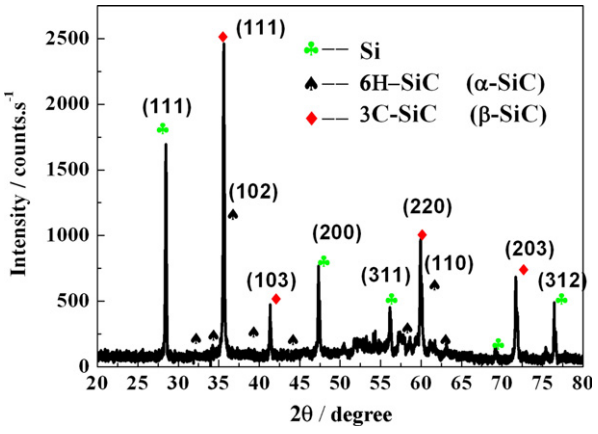

Fig. 3. XRD pattern for RBSC prepared with $P_{1.2}$:C = 40:60.

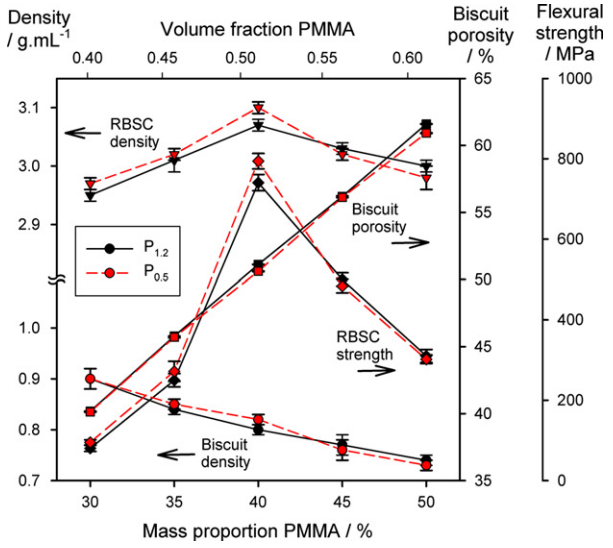

Fig. 4. Variation of flexural strength and density of RBSC ceramics, and density and porosity of the carbon biscuit, with mass proportion of PMMA.

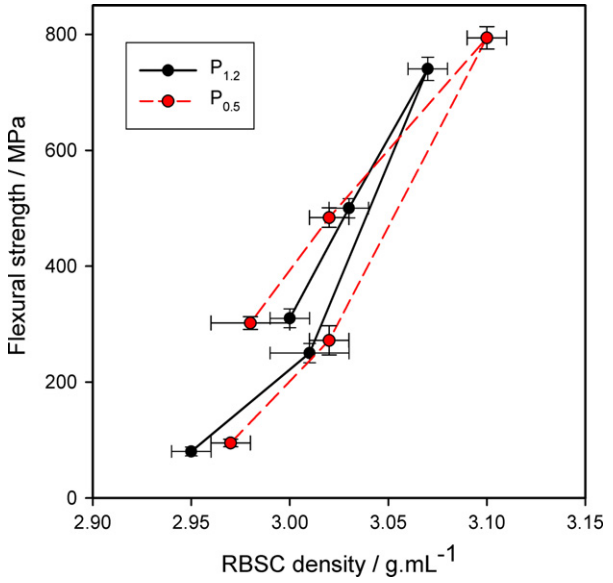

Fig. 5. Relationship of the flexural strength of RBSC ceramics to density.

mechanical properties of RBSC are affected by the porosity and microstructure of the carbon biscuit as well as the volume fractions of C_R and Si_R.

Even so, the mechanical properties of the RBSC ceramics are difficult to predict on a "rules of mixtures" basis because only empirical equations are available for some composite systems, although porosity, as flaws in the Griffith sense, would be expected to be a dominant factor. But both C_R and Si_R are substantially weaker than SiC, and thus, if present, grains of these materials would be expected to reduce the flexural strength of the composite as if they were pores themselves. Accordingly, when either C or Si is in excess, a steep fall in strength is expected from the cusp corresponding to pure SiC (and is thus the cause of the problem with "black core"). This is essentially what is seen in Fig. 4. The cusp, however, is not symmetrical, presumably because the carbon is inherently weaker than solid silicon. The experimental optimum here is seen to lie close to P:C=40:60. This also corresponds to a peak in density (Figs. 4 and 5).

3.3. Effect of PMMA content and particle size on the microstructure of RBSC

Fig. 6 shows optical micrographs of RBSC ceramics prepared with $P_{1.2}$ and $P_{0.5}$. For $P_{1.2}$, as P:C increased from 30:70 to 35:65, the particle size of C_R (dark phase in Fig. 6a1–b1) decreased from ~4 μm to less than ~2 μm; the amount also decreased; at P:C=40:60 (biscuit density ρ_b=0.82 g/mL) and above, no C_R was detectable. Previously, it had been reported that this critical value was 0.81 g/mL [22], while we had earlier attained 0.84 g/mL [23].

The amount of Si_R increased with P:C ratio, its distribution varying from isolated to continuous (pale phase in Fig. 6a1–e1). At low P:C ratio, the Si_R distribution was uniform and the amount very low, grains being $\leq$1 μm. However, increasing P:C over 50:50 gave a sharp increase in both the content and grain size of Si_R, reaching 2–3 μm.

In comparison, for $P_{0.5}$, the grain size of C_R was clearly smaller (Fig. 6a2–b2), while both the amount and grain size of the Si_R also decreased, with a more uniform distribution, this uniformity persisting up to P:C=50:50 (Fig. 6a2–e2). However, for P: C=50:50, some larger grains appeared which may have been due to agglomeration of smaller PMMA particles (this effect was more apparent in work at higher ratios (not shown)). This may mean that some better dispersant may be required to ensure uniformity.

"Black core" C_R in the RBSC was clearly controllable through the P:C ratio, as would be expecting from the stoichiometry of the reaction; the absence at P:C=40:60 and above suggests that sufficient intimacy of the infiltrated mixture has occurred to yield esssentially complete reaction, thus the detrimental "black core" can be effectively avoided with the process used here.

3.4. Effect of carbonization process on property of biscuit

Thermal decomposition of $P_{1.2}$ occurred at 250–400 °C, giving a rapid mass loss of about 90% (Fig. 7). Above this temperature, the mass loss was more gradual, the rate increasing again from 630 to 760 °C, and corresponding to an exotherm, the cause of which is unclear. Overall, the mass retention was only 0.08 mass% by 760 °C. Up to 400 °C, the behavior was similar to that seen elsewhere [24]. Nevertheless, it was found that there was continuous volumetric shrinkage of the carbon biscuit above 400 °C, perhaps due to a sintering process. To obtain a fully volume-stable biscuit of constant mass, heating to 800–1000 °C was required. Since "unzipping" depolymerization to yield

high-purity methyl methacrylate is the normal process, the pyrolysis products obtained from the present "carbonization" process might be worth checking (better renamed simply as pyrolysis here since no carbon is meant to arise from the PMMA) to establish the cause of the difference although this is likely to be due to the poly(vinylpyrrolidone) used (and thus also the unexplained exotherm). Even so, the low residue confirms that PMMA is well suited as a pore former in this context. The residue has not been taken into account now.

During both the pyrolysis and the infiltration the heating rate should be kept low. It was found that obvious microcracks would occur in the biscuit, for example, if the temperature was increased at >20 K/min (from room temperature to 1000 °C), giving rise to the appearance of "silicon wire" in the RBSC (Fig. 8; *i.e.*, an infiltrated crack in cross-section). A rate of 10 K/min was chosen for a margin of safety, and no such cracks were detected in any resulting ceramic.

3.5. Residual carbon

"Black core" in RBSC ceramics often occurs after liquid silicon infiltration primarily when there is excess C with respect to the stoichiometry of SiC, but also possibly due to blockage of some more capillary-like connecting porosity due to a volumetric expansion on reaction. Washburn [25] studied the penetration of liquids into cylindrical capillaries and found that infiltration depth (x) and time (t) had a parabolic relationship, dependent on fluid viscosity (μ), and surface tension (γ), capillary radius (r),

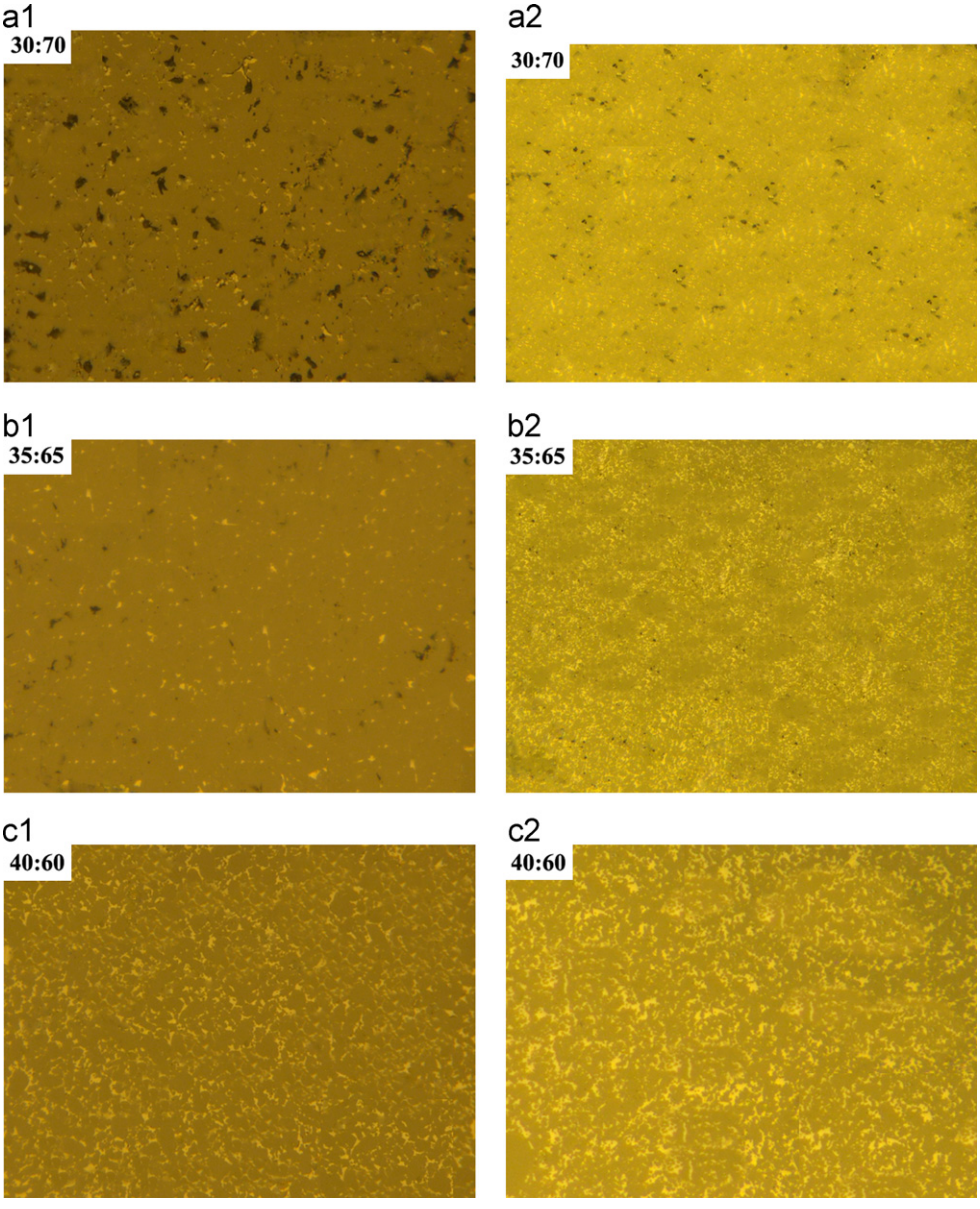

Fig. 6. Optical micrographs of RBSCs prepared with $P_{1.2}$ (a1)–(e1) and $P_{0.5}$ (a2)–(e2). Mass ratios (P:C): a—30:70, b—35:65, c—40:60, d—45:55 and e—50:50.

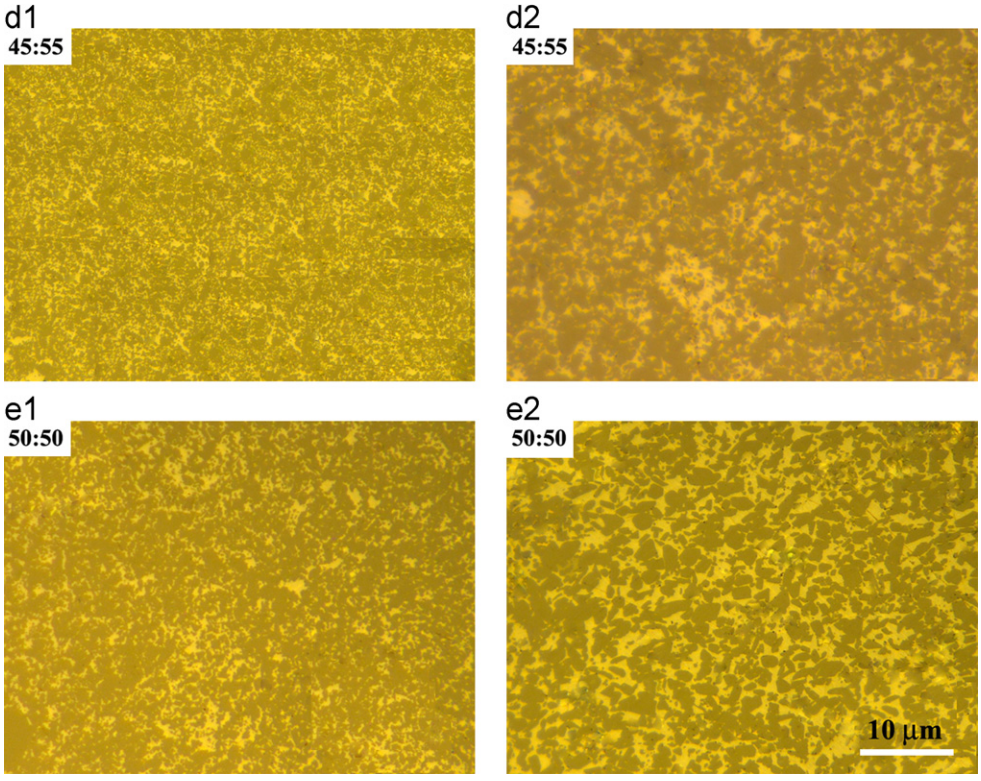

Fig. 6. Continued.

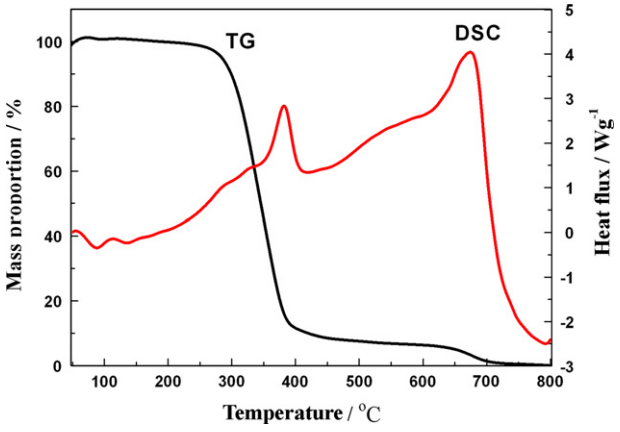

Fig. 7. TG/DSC curves for $P_{1.2}$.

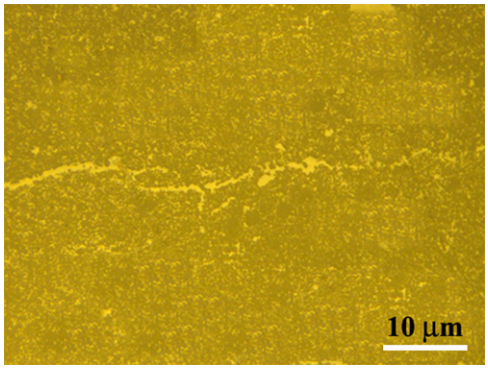

Fig. 8. Optical micrograph of RBSC prepared with $P_{1.2}$:C=40:60 biscuit pyrolysed at a heating rate of 20 K/min.

and the contact angle (θ) of the fluid on the wall:

$$\frac{x}{\sqrt{t}} = \frac{\gamma \cos\theta}{\mu} r \quad (1)$$

Despite a number of assumptions, this equation has found wide acceptance also for modeling the infiltration depth in porous bodies. Thus here, for biscuits of the same density, the infiltration rate of the molten silicon is increased for large C particles as these give large spaces between and thus large equivalent capillary radii. However, for such carbon powders, the forming β-SiC will deposit as a thickening layer around the carbon particles. This layer will then tend to occlude the infiltration pathways, but also kinetically limit access of the Si to remaining C, thus leading to the presence of unreacted carbon (and also possibly of Si) in the resulting RBSC ceramics [8].

Using PMMAs with a relatively narrow particle size dispersion as a pore former, the porosity was reasonably homogeneous, an essential condition for complete infiltration. For P:C > 40:60, the porosity of the biscuit was > 50%, which should provide enough connected capillary apertures to favor the infiltration, allowing the carbon to be reacted completely, with little capillary obstruction; thus, "black core" was not detectable at high enough P:C ratios (Fig. 6c1–e1). Further, reducing the particle size of the PMMA reduced both the content and grain size of Si_R,

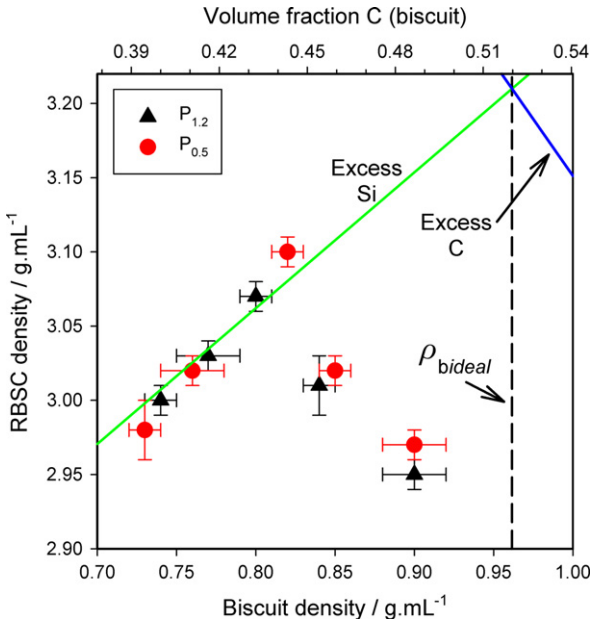

Fig. 9. Density of RBSC ceramics with respect to that of biscuit in relation to ideal outcome for excess Si, perfect conversion, and excess C.

but still homogeneously (Fig. 6a2–e2). For P:C < 40:60, the biscuits had a relatively high ρ_b and low porosity, and the carbon powder used in this work could give rise to high ρ_b locally due to agglomeration (Fig. 6a1–b1). The molten silicon hardly infiltrated into parts of the biscuits in such cases, leaving large areas of "black core" (Fig. 6a1 and a2).

The conversion of C to SiC is said to involve a change of the total volume of solid of some 2.0–2.2 fold [26]. This is defined by the molar volume ratio:

$$\text{volume ratio} = \frac{\rho_C}{\rho_{SiC}}\frac{M_{SiC}}{M_C} \tag{2}$$

where M is the molar mass of the subscripted substance, and $\rho_{SiC}=3.21$ g/mL, with $\rho_C=1.85$ g/mL for the source carbon, which gives the value 1.92 here. As indicated above, this solidification tends to block capillaries and thus the continued infiltration of molten silicon, leaving residual carbon in the RBSC, quite apart from any stoichiometric considerations.

3.6. Control of the biscuit density

The carbon density of the biscuit is the key factor for the quality of the resulting RBSC ceramic. If SiC is the only phase present (no pores, Si_R or C_R), the theoretically required biscuit density $\rho_{b\,ideal}=0.962$ g/mL is given by

$$\rho_{b\ ideal} = \rho_{SiC}\frac{M_C}{M_{SiC}} \tag{3}$$

on the basis of (bulk) molar volume equality, there being no overall volume change. This gives a slightly different result from that previously reported [15]:

$$\rho_{b\ ideal} = \frac{\rho_{SiC}}{1+\rho_{Si}} \tag{4}$$

the reasoning for which is not clear. If there is excess Si, and thus Si_R is present, the theoretical density of the RBSC (*i.e.* no C_R and porosity zero), is given by

$$\rho_{RBSC} = \rho_b\frac{M_{SiC}}{M_C} + \rho_{Si}\left(1-\frac{M_{SiC}}{M_C}\frac{\rho_b}{\rho_{SiC}}\right) \tag{5}$$

where ρ_b is the actual carbon biscuit density, and $\rho_{Si}=2.33$ g/mL which reduces to [23]

$$\rho_{RBSC} = 2.33+0.9158\rho_b \tag{6}$$

Likewise, if there is excess C, and thus C_R is present ($\rho_{CR}=1.85$ g/mL, assuming change of the source carbon), we have

$$\rho_{RBSC} = \rho_b + \frac{\rho_{SiC}M_{Si}(\rho_b-\rho_{C_R})}{\rho_{SiC}M_C-\rho_{C_R}M_{SiC}} \tag{7}$$

which reduces to

$$\rho_{RBSC} = 4.68198-1.5308\rho_b \tag{8}$$

The intersection of (6) and (8) is at the value of (3). These calculations allow assessment of the efficacy of the present method (Fig. 9). The present data fit fairly well the "excess Si" prediction, but clearly do not approach ideality. Even so, at $P_{0.5}$:C=40:60, the relative density of the RBSC ceramic was ~96.6%, which appears to be responsible for the high strength. Whether it is possible to improve on this can now be explored, primarily through improving the critical biscuit density and reaction completion. That there is scope for this is apparent since it is clear from Fig. 6(a, b) that both C_R and Si_R are present at the higher values of ρ_b.

4. Conclusions

RBSC ceramics with high density and flexural strength were successfully prepared by adjusting the proportion of PMMA powder in the green body. Residual carbon – "black core" – was effectively eliminated for 40 mass% PMMA and above. The value of the optimum ratio can now be refined. Using the smaller particle-size PMMA was favorable in terms of Si_R grain size and improved both density and flexural strength in the RBSC ceramic. The "silicon wire" cracking defect can be avoided by slow heating. The observed agglomeration of fine powders requires the identification of better dispersants or dispersion techniques.

Acknowledgment

This work was supported by the Fundamental Research Funds for the Central Universities of China (No. 2011-IV-133).

References

[1] W. Yao, Y.M. Zhang, J.C. Han, H.B. Zuo, Fabrication and test of reaction bond silicon carbide for optical applications, Transactions of Nonferrous Metals Society of China 16 (2006) 409–413.

[2] S. Suyama, T. Kameda, Y. Itoh, Development of high-strength reaction-sintered silicon carbide, Diamond and Related Materials 12 (2003) 1201–1204.
[3] C. Santos, C.A. Kelly, S. Ribeiro, K. Strecker, J.V.C. Souza, O.M.M. Silva, α-Sialon–SiC composites obtained by gas-pressure sintering and hot-pressing, Journal of Materials Processing Technology 189 (2007) 138–142.
[4] G. Magnani, L. Beaulardi, L. Pilotti, Properties of liquid phase pressureless sintered silicon carbide obtained without sintering bed, Journal of the European Ceramic Society 25 (2005) 1619–1627.
[5] A. Gubernat, L. Stobierski, P. Łabaj, Microstructure and mechanical properties of silicon carbide pressureless sintered with oxide additives, Journal of the European Ceramic Society 27 (2007) 781–789.
[6] G. Magnani, G.L. Minoccari, L. Pilotti, Flexural strength and toughness of liquid phase sintered silicon carbide, Ceramics International 26 (2000) 495–500.
[7] L. Esposito, D. Sciti, A. Piancastelli, A. Bellosi, Microstructure and properties of porous β-SiC templated from soft woods, Journal of the European Ceramic Society 24 (2004) 533–540.
[8] Y.M. Chiang, R.P. Messner, C.D. Terwilliger, D.R. Behrendt, Reaction-formed silicon carbide, Materials Science and Engineering: A 144 (1991) 63–74.
[9] E.E. Hucke, Methods of producing carbonaceous bodies and the products thereby, US Patent 3859421, 1975.
[10] Z. Yan, J. Liu, J. Zhang, T. Ma, Z. Li, Biomorphic silicon/silicon carbide ceramics from birch powder, Ceramics International 37 (2011) 725–730.
[11] Z. Yan, J. Liu, J. Zhang, T. Ma, Z. Li, Comparative study of biomorphic silicon/silicon carbide ceramic from birch and compressed birch, Key Engineering Materials 434–435 (2010) 609–612.
[12] K.E. Pappacena, S.P. Gentry, T.E. Wilkes, M.T. Johnson, S. Xie, A. Davis, et al., Effect of pyrolyzation temperature on wood-derived carbon and silicon carbide, Journal of the European Ceramic Society 29 (2009) 3069–3077.
[13] D. Mallick, O.P. Chakrabarti, H.S. Maiti, R. Majumdar, Si/SiC ceramics from wood of Indian dicotyledonous mango tree, Ceramics International 33 (2007) 1217–1222.
[14] N.R. Calderon, M. Martinez-Escandell, J. Narciso, F. Rodríguez-Reinoso, The role of carbon biotemplate density in mechanical properties of biomorphic SiC, Journal of the European Ceramic Society 29 (2009) 465–472.
[15] P. Popper, The preparation of dense self-bonded silicon carbide, in: P. Popper (Ed.), Special Ceramics, Heywood, London. 1960, pp. 209–219.
[16] Y.H. Chen, Y.Y. Liu, R.H. Lin, F.-S. Yen, Characterization of magnetic poly(methyl methacrylate) microspheres prepared by the modified suspension polymerization, Journal of Applied Polymer Science 108 (2008) 583–590.
[17] Z.Z. Gu, H. Chen, S. Zhang, L. Sun, Z. Xie, Y. Ge, Rapid synthesis of monodisperse polymer spheres for self-assembled photonic crystals, Colloids and Surfaces A: Physicochemical and Engineering Aspects 302 (2007) 312–319.
[18] J. Safarian, B. Xakalashe, M. Tangstad. Vacuum removal of the impurities from different silicon melts. in Proceedings of the 26th European Photovoltaic Solar Energy Conference and Exhibition, Hamburg, Germany, 2011.
[19] P.D. Desai, Thermodynamic properties of iron and silicon, Journal of Physical and Chemical Reference Data 15 (1986) 967–983.
[20] T. Hase, H. Suzuki, T. Iseki, Formation process of β-SiC during reaction-sintering, Journal of Nuclear Materials 59 (1976) 42–48.
[21] D.H. Kim, C.H. Kim, Toughening behavior of silicon carbide with additions of yttria and alumina, Journal of the American Ceramic Society 73 (1990) 1431–1434.
[22] R.P. Messner, Formation Kinetics of Reaction Bonded Silicon Carbide Based Materials, Ph.D. Dissertation, Massachusetts Institute of Technology, Cambridge, Massachusetts, USA, 1991.
[23] Q. Wu, Y. Yan, X. Zhao, B. Guo, M. Li, X. Liu, Research on the sintering of reaction bonded silicon carbide with pure carbonaceous preform, Journal of Wuhan University of Technology 25 (2003) 1–3.
[24] L.A. Salam, R.D. Matthews, H. Robertson, Pyrolysis of poly-methyl methacrylate (PMMA) binder in thermoelectric green tapes made by the tape casting method, Journal of the European Ceramic Society 20 (2000) 335–345.
[25] E.W. Washburn, The dynamics of capillary flow, Physical Review 17 (1921) 273–283.
[26] Q. Wu, X. Wu, Q. Zhu, N. Li, Study on preparation of reaction burning silicon carbide by carbon powder, Journal of Wuhan University of Technology—Materials Science Edition 12 (1997) 35–40.